Inorganic Chemistry

Article

pubs.acs.org/IC

$La_3Ni_2SbO_9$: a Relaxor Ferromagnet

Peter D. Battle,* Sophie I. Evers, Emily C. Hunter, and Mark Westwood

Inorganic Chemistry Laboratory, University of Oxford, South Parks Road, Oxford, OX1 3QR, U. K.

Supporting Information

ABSTRACT: A polycrystalline sample of $La_3Ni_2SbO_9$ has been synthesized using a standard ceramic method and characterized by neutron diffraction and magnetometry. The compound adopts a monoclinic, perovskite-like structure with space group $P2_1/n$ and unit cell parameters a = 5.0675(1), b = 5.6380(1), c = 7.9379(2) Å, β = 89.999(6)° at room temperature. The two crystallographically distinct six-coordinate sites are occupied by Ni^{2+} and a disordered distribution of Ni^{2+}/Sb^{5+}, respectively; the Ni^{2+} and Sb^{5+} cations occupy the disordered site in a 1:2 ratio. Both ac and dc magnetometry indicate the presence of a spontaneous magnetization below 105 K. A magnetization of 1.5 μ_B per formula unit was measured at 2 K in a field of 40 kOe. However, no magnetic scattering was observed in neutron diffraction data collected at 5 K. It is proposed that, as a consequence of the cation disorder, $La_3Ni_2SbO_9$ behaves as a relaxor ferromagnet, analogous to a relaxor ferroelectric, with magnetic domains too small to be detected by neutron diffraction forming below 105 K.

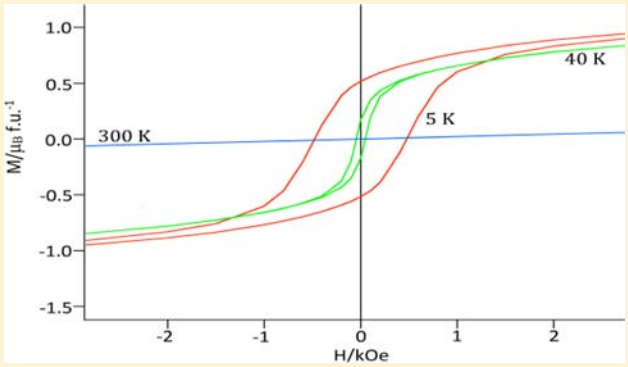

INTRODUCTION

The perovskite structure has been central to the development of inorganic magnets and dielectrics for many years. The structure is remarkably flexible and can consequently accommodate a variety of elements which between them cover a wide range of ionic size and charge. The properties of a particular composition ABO_3 depend on the electron configuration of the cations A and B. When the compound is intended for use as a dielectric, a diamagnetic cation, often having a lone-pair of electrons in the valence shell, for example, Pb(II) or Bi(III), is chosen to occupy the A site. B, the smaller of the two cations, is usually a transition metal in its highest accessible oxidation state, for example, Nb(V); the valence-shell electron configuration in this case is d^0. At some critical temperature, these perovskites may undergo a structural phase transition which results in the formation of a so-called ferroelectric phase with a net electrical polarization. When it is the magnetic properties that are of interest, B is usually a paramagnetic transition-metal cation with a partially filled d shell. In this case, the magnetic properties may be enhanced if the larger cation, A, is also paramagnetic. Below some critical temperature the atomic moments of the paramagnetic cations can align parallel to each other to form a ferromagnetic ground state with a spontaneous magnetization, although antiparallel alignment to form a less-useful antiferromagnetic ground state with no net magnetization is more common. There are clearly parallels between these two types of "ferroic" systems, but there are very few materials that are both ferromagnetic and ferroelectric, that is "multiferroic"; the reasons for this lack of overlap have been discussed by Hill.[1]

The description of ferroelectrics and ferromagnets given above is very simplistic, and many variations on the principal theme have been reported. One of the most widely reported variations involves compounds in which either the B site or both the B site and the A site are occupied by two distinct cation species in varying ratios, thus leading to formulas of the type $A_2BB'O_6$, $AA'BB'O_6$ or, $A_2A'B_2B'O_9$.[2] It has been shown that the physical properties of these more complex compositions are largely determined by the extent to which B and B' are ordered over the six-coordinate sites. In the magnetic case, an ordered arrangement usually leads to the adoption of a ground state that shows long-range magnetic order, as in Ba_2NiWO_6,[3,4] whereas a disordered arrangement can result in the formation of a spin glass, as in Sr_2FeTaO_6.[5,6] In the case of dielectrics, a particularly interesting type of behavior has been observed in a number of disordered $A_3B_2B'O_9$, compositions, often written as $A(B_{2/3}B'_{1/3})O_3$ to emphasize the lack of complete cation order on the six-coordinate sites. It has been shown[7] that the crystal structure of $Pb(Mg_{1/3}Nb_{2/3})O_3$, for example, contains two crystallographically distinct, six-coordinate sites which form interpenetrating face-centered cubic (fcc) arrays in a unit cell with a lattice parameter double that of the simple perovskite unit cell. One of these fcc sublattices is occupied exclusively by the "electrically-active" d^0 Nb(V) species whereas the other is occupied by a disordered distribution of Mg(II) and Nb(V) in a 2:1 ratio. Thus the compound shows as much cation order as is possible when the structure contains two sites with equal multiplicities that must

Received: March 19, 2013
Published: May 20, 2013

be occupied by two different cation species in a 2:1 ratio. Indeed, the structure has been described as 1:1 ordered, even though occupational disorder is present on one of the two sites. This cation distribution results in the formation of what has become known as a "relaxor ferroelectric" in which ferroelectric domains exist in a paraelectric matrix.[8] The formation of these domains, which stems from the residual cation disorder in the structure, can be recognized experimentally by the occurrence of a broad, frequency-dependent maximum in the temperature dependence of the dielectric constant, a signature analogous to that shown by the magnetic susceptibility of spin glasses. Relaxor ferroelectrics have been the subject of much research activity, some of which has recently been reviewed by Cowley et al.[9]

In the light of the analogy between ferromagnets and ferroelectrics drawn above, it is interesting to consider whether the comparison can be extended to include relaxors. The term "relaxor ferromagnet" has been used previously[10] to describe the behavior of $Nd_{0.5}Ca_{0.5}MnO_3$ when doped with ~2% Cr^{3+}; ferromagnetic, metallic domains form within the antiferromagnetic, charge-ordered structure of the undoped material. In the belief that it should be possible to produce a magnetic analogue of the relaxor ferroelectric in which the behavior stems from the properties of the bulk material, rather than from a dopant, we have undertaken an investigation of $La_3Ni_2SbO_9$. In this compound the A sites are all occupied by spherical La^{3+} cations, and the B and B' sites are occupied by Ni(II):d^8 and Sb(V):d^{10} cations in a 2:1 ratio. On the basis of direct current (dc) susceptibility data, Alvarez et al.[11] have previously concluded that a spin-canted antiferromagnetic phase is formed at low temperatures.

EXPERIMENTAL SECTION

A polycrystalline sample of $La_3Ni_2SbO_9$ was prepared by firing stoichiometric quantities of Sb_2O_5, NiO and predried La_2O_3 at 1250 °C for six days in an alumina crucible. The reactants were finely ground in an agate mortar and pestle and then pelletized. The pellets were ground and reformed every 2 days. A Philips X'Pert Pro X-ray powder diffractometer was used to monitor the progress of the reaction. Data collected at room temperature using Cu Kα_1 radiation were analyzed by the Rietveld method as implemented in the GSAS program suite.[12,13] Neutron powder diffraction data were collected over the angular range $10 \leq 2\theta/° \leq 160$ at selected temperatures using the diffractometer D2b at ILL, Grenoble. Data were collected using neutron wavelengths of 1.594 and 2.4 Å as detailed below. The sample was contained in a vanadium can of diameter 8 mm that was mounted in a standard ILL cryostat for experiments below room temperature; profile points contaminated by scattering from the cryostat (2θ >150° for λ = 1.594 Å) were excluded from the analysis.

The magnetic properties of $La_3Ni_2SbO_9$ were measured using a Quantum Design SQUID magnetometer. The dc magnetic susceptibility was measured while warming the sample through the temperature range $5 \leq T/K \leq 300$ in a field of 100 Oe; data were collected after cooling the sample to 5 K in the absence of an applied field (ZFC) and after cooling the sample in the measuring field (FC). The isothermal sample magnetization was measured as a function of field over the range $-50 \leq H/kOe \leq 50$ at selected temperatures. The sample was cooled to the measuring temperature in a field of 50 kOe. The alternating current (ac) susceptibility was measured at frequencies of 1, 10, 100, and 1000 Hz over the temperature range $70 \leq T/K \leq 110$ in an oscillating field of amplitude 3.5 Oe.

RESULTS

The X-ray diffraction pattern of the final reaction product indicated that a pseudocubic perovskite phase had formed, together with a small amount of La_3SbO_7, and that some unreacted nickel oxide remained. Rietveld refinement of the structure in space group $P2_1/n$ confirmed this and quantified the impurity levels as 0.49(6) and 0.77(5) wt % of NiO and La_3SbO_7, respectively. Analysis of neutron diffraction data collected at room temperature using a wavelength λ = 1.594 Å resulted, as expected, in a more precise structure refinement. Preliminary refinements showed that one of the six-coordinate sites, Ni/Sb1, was occupied only by nickel while the other was occupied by a disordered 2:1 distribution of Sb and Ni. This result was used to constrain the cation distribution in our final analyses. No Bragg peaks attributable to NiO or La_3SbO_7 were apparent in the neutron data. The structural parameters derived from these data are presented in Table 1, and the corresponding bond lengths and angles are listed in Table 2. The observed and calculated diffraction profiles are shown in Figure 1, and the extent of the distortion away from cubic symmetry can be gauged from the tilting of the octahedra apparent in Figure 2. The structural parameters and bond lengths derived from data collected at 5 K using a wavelength of 1.594 Å are also included in Tables 1 and 2, respectively. No additional Bragg peaks attributable to the adoption of a magnetically ordered ground state were apparent in these data. To confirm the absence of magnetic Bragg peaks, an additional diffraction pattern was collected at 5 K using a wavelength of 2.4 Å. These data did not reveal any additional Bragg peaks at the relatively high d spacings that are sampled at 2.4 Å but not at 1.594 Å, see Supporting Information, Figure S1. Any magnetic contributions to the structural Bragg peaks were too

Table 1. Structural Parameters of $La_3Ni_2SbO_9$ at Room Temperature and 5 K (Space Group $P2_1/n$)

		room temperature	5 K
a/ Å		5.6075(1)	5.5972(2)
b/ Å		5.6380(1)	5.6346(1)
c/ Å		7.9379(2)	7.9248(2)
β/ deg		89.999(6)	90.005(7)
R_{wp}		0.044	0.045
χ^2		4.416	6.800
La	x	0.4908(6)	0.4911(5)
4e (x y z)	y	0.4632(2)	0.46010(2)
	z	0.252(1)	0.2481(10)
	U_{iso}/Å^2	0.0204(4)	0.0147(4)
Ni/Sb1	U_{iso}/Å^2	0.0051(8)	0.0005(7)
2c (0 $^1/_2$ 0)	Ni occupancy	1	1
	Sb occupancy	0	0
Ni/Sb2	U_{iso}/ Å^2	0.0014(10)	0.00010(10)
2d ($^1/_2$ 0 0)	Sb occupancy	0.6667	0.6667
	Ni occupancy	0.3333	0.3333
O1	x	0.787(1)	0.788(1)
4e (x y z)	y	0.7976(9)	0.7972(10)
	z	−0.0470(6)	−0.0479(6)
	U_{iso}/Å^2	0.011(1)	0.006(1)
O2	x	0.709(1)	0.7010(1)
4e (x y z)	y	0.2845(10)	0.285(1)
	z	−0.0387(6)	−0.0388(7)
	U_{iso}/Å^2	0.004(2)	0.002(2)
O3	x	0.5761(5)	0.5775(5)
4e (x y z)	y	0.0171(4)	0.0176(4)
	z	0.245(1)	0.249(1)
	U_{iso}/ Å^2	0.0111(5)	0.0082(5)

dx.doi.org/10.1021/ic400675r | Inorg. Chem. 2013, 52, 6648−6653

Table 2. Bond Lengths (Å) and Bond Angles (deg) in $La_3Ni_2SbO_9$ at Room Temperature and 5 K

	room temperature	5 K
Ni/Sb1−O1	2.094(5)	2.088(5)
Ni/Sb1−O2	2.055(6)	2.050(6)
Ni/Sb1−O3	2.071(10)	2.036(10)
Ni/Sb2−O1	2.007(6)	2.011(5)
Ni/Sb2−O2	2.012(6)	2.012(5)
Ni/Sb2−O3	1.993(10)	2.025(10)
La−O1	2.815(9)	2.833(8)
La−O1	2.687(7)	2.658(7)
La−O1	2.384(8)	2.401(8)
La−O2	2.799(9)	2.767(9)
La−O2	2.478(8)	2.463(8)
La−O2	2.686(8)	2.693(8)
La−O3	2.561(2)	2.545(3)
La−O3	2.448(4)	2.463(4)
O1−Ni/Sb1−O2	89.7(3)	89.8(3)
O1−Ni/Sb1−O3	91.1(2)	91.0(2)
O2−Ni/Sb1−O3	90.6(2)	90.3(2)
O1−Ni/Sb2−O2	87.6(3)	87.5(3)
O1−Ni/Sb2−O3	92.2(2)	92.4(2)
O2−Ni/Sb2−O3	89.2(2)	89.2(2)

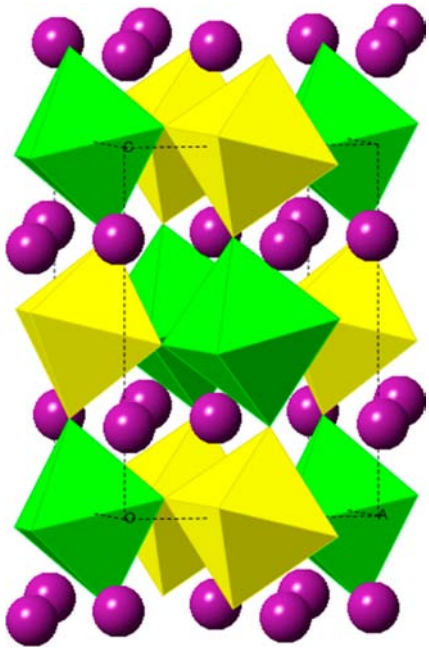

Figure 2. Crystal structure of $La_3Ni_2SbO_9$. Green and yellow octahedra represent NiO_6 and Ni/SbO_6 groups, respectively. Purple circles represent La^{3+} cations.

weak to be detected, and the data collected at 5K were consequently analyzed using a nonmagnetic model. The fitted diffraction pattern is shown in Supporting Information, Figure S2.

The temperature dependence of the dc molar magnetic susceptibility, see Figure 3, increases sharply at 100 K, and the data collected under ZFC and FC conditions do not coincide at lower temperatures. Fitting the data collected in the temperature range $200 < T/K < 300$ to the Curie−Weiss law gave an effective magnetic moment of 2.2(1) μ_B per Ni^{2+} cation and a Weiss temperature $\theta = 159$ K. The ac susceptibility, see Figure 4, is frequency dependent and has a nonzero imaginary component below 105 K. The transition temperature is independent of the measuring frequency. The function $M(H)$, see Figure 5, appears linear in low fields at 140 K, but a deviation from paramagnetic behavior is seen for $H > 20$ kOe; hysteresis is clearly seen in low fields at 40 and 5 K. The magnetization approaches a saturation value of ~1.5 μ_B per formula unit (f.u.) in 40 kOe at 5 K, with a remanent magnetization of 0.5 μ_B per f.u. and a coercive field of 500 Oe.

DISCUSSION

The type of monoclinic crystal structure described in Tables 1 and 2 and illustrated in Figure 2 is common among perovskites, including $SrLaNiSbO_6$,[14] that contain two species of six-coordinate cations in a 1:1 ratio. It is less common among those

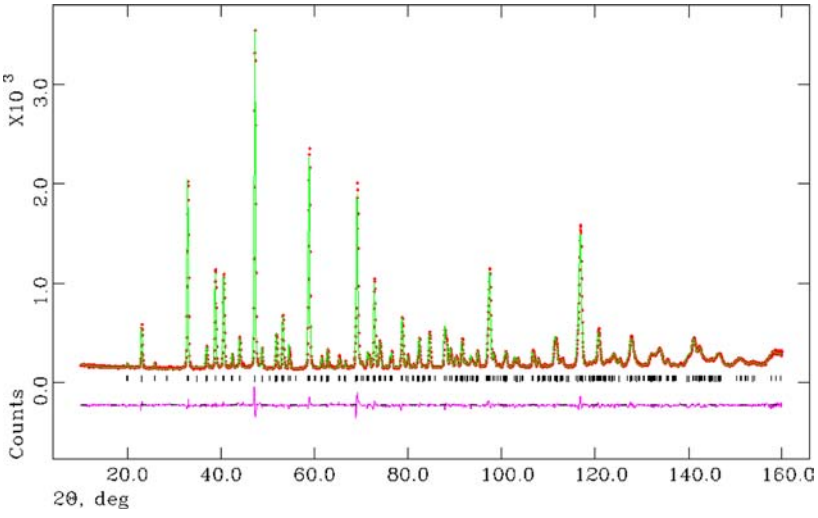

Figure 1. Observed (red solid circles) and calculated (green line) neutron diffraction patterns for $La_3Ni_2SbO_9$ at room temperature. A difference plot is shown and reflection positions are marked by vertical bars.

dx.doi.org/10.1021/ic400675r | Inorg. Chem. 2013, 52, 6648−6653

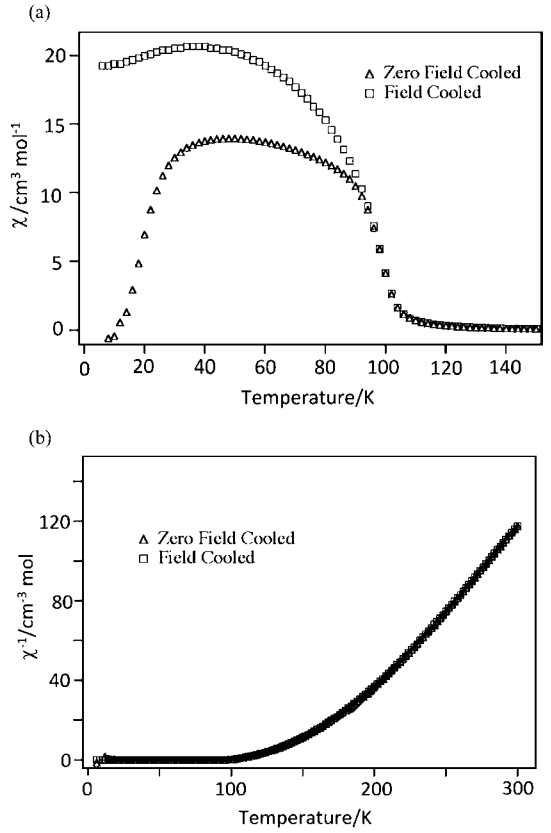

Figure 3. Temperature dependence of (a) the molar magnetic susceptibility (M/H) of $La_3Ni_2SbO_9$ and (b) the inverse molar susceptibility.

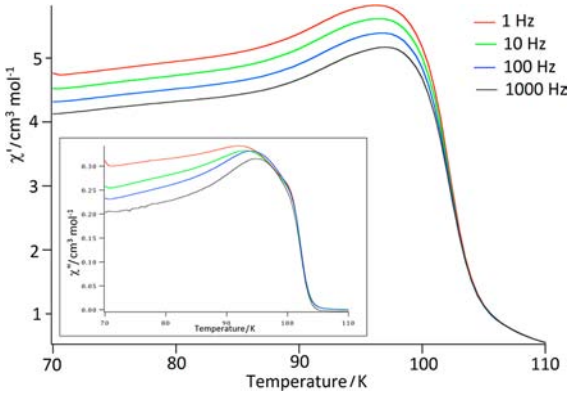

Figure 4. Temperature and frequency dependence of the real and imaginary parts of the ac susceptibility of $La_3Ni_2SbO_9$. Data collected at 1, 10, 100, and 1000 Hz are shown in descending order.

in which these cations occur in a 2:1 ratio. In $SrLaNiSbO_6$ the Ni^{2+} and Sb^{5+} cations were found to be partially ordered with mean metal-to-oxygen bond lengths of 2.056 and 1.992 Å on the sites occupied by 90% Ni^{2+} and Sb^{5+}, respectively. The mean bond lengths at the Ni/Sb1 and Ni/Sb2 sites in $La_3Ni_2SbO_9$ at room temperature are 2.073 and 2.004 Å respectively, the increases reflecting the fact that both sites have a relatively high Ni^{2+} content. We note that the Ni−O bond length in NiO is 2.089(5) Å,[15] and the mean Sb−O distance in Sb_2O_5 is 1.992 Å.[16] Some of the tabulated structural parameters require comment. The value of the unit cell parameter β is very close to 90°. However, attempts to refine the structure in an

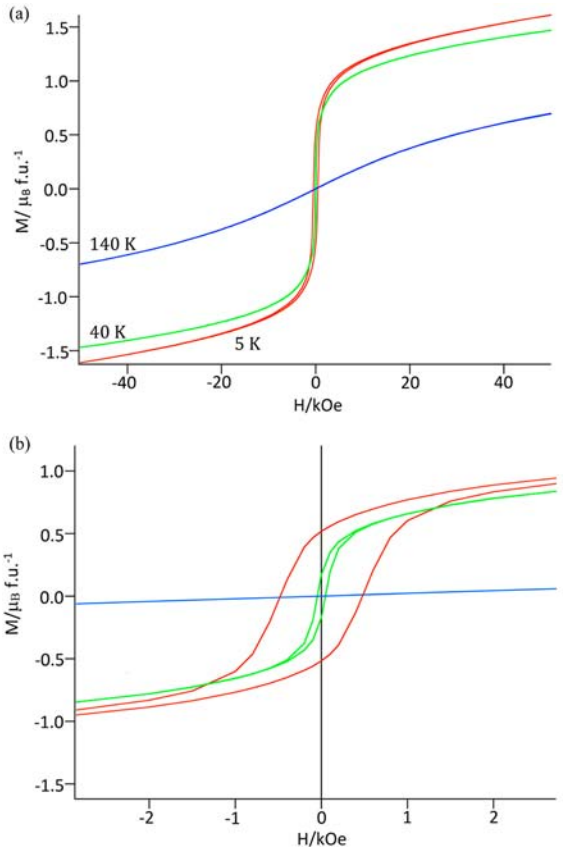

Figure 5. Field dependence of the magnetization per formula unit of $La_3Ni_2SbO_9$ at 5 K (red), 40 K (green), and 140 K (blue).

orthorhombic space group were unsuccessful, and we conclude that although the unit cell might be close to orthorhombic metrically, the symmetry of the atomic arrangement within the cell is indeed monoclinic. The majority of the structural parameters presented in Table 1 are unremarkable, but the atomic displacement parameter of the La^{3+} cations is unusually large. The value decreases by ∼25% on cooling from room temperature to 5 K, but the value of 0.0147(4) obtained at the lower temperature is large enough to suggest that the atomic disorder on the Ni/Sb2 site induces a degree of static disorder around the *A* site.

The magnetic data shown in Figures 3, 4, and 5 add much to those published previously.[11] They suggest that $La_3Ni_2SbO_9$ adopts a ferromagnetic or ferrimagnetic ground state below ∼100 K. The effective magnetic moment above the Curie temperature is unusually low for Ni^{2+}, but this might be ascribed to our use of the Curie−Weiss law in a temperature region wherein the sample is not behaving as a true paramagnet. The observation[17] of antiferromagnetic ordering below 275 K in the perovskite $KNiF_3$ suggests that short-range antiferromagnetic coupling will indeed be present in $La_3Ni_2SbO_9$ over the measured temperature range. The magnetization does not achieve saturation in a field of 40 kOe, but it appears that the saturation magnetization is likely to be ∼1.6 μ_B per formula unit. The magnetic cations in this compound can be considered to form a primitive pseudocubic array in which alternate sites have 100% and 33% probabilities of being occupied by a magnetic cation. The superexchange coupling, parametrized by J_1, between Ni^{2+} cations on nearest-neighbor (NN) sites is expected to be the strongest magnetic

dx.doi.org/10.1021/ic400675r | Inorg. Chem. 2013, 52, 6648−6653

interaction, and NN Ni^{2+} cations in a simple cubic lattice are expected to couple antiferromagnetically, as exemplified by $KNiF_3$.[18] However, one of these sites has only a 33% probability of being occupied by Ni^{2+}, and the resulting imbalance between the number of spin-up and spin-down cations results in ferrimagnetism rather than antiferromagnetism. If each cation has an ordered moment of M_{Ni} μ_B, then the magnitude of the net magnetization per formula unit is predicted to be $(1.5M_{Ni}-0.5M_{Ni}) \sim 1.6$ μ_B. Hence $M_{Ni} \sim 1.6$ μ_B, a value that is slightly lower than that expected for an $S = 1$ cation ($M \sim 2$ μ_B). However, this model must be an oversimplification because it describes a ferrimagnetic ground state with long-range magnetic order that would result in magnetic Bragg scattering in the neutron diffraction pattern collected at 5 K. To account for the apparent absence of any such scattering it is necessary to consider the significance of other antiferromagnetic superexchange interactions, see Figure 6. These are most likely to be important when a local region of

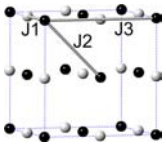

Figure 6. Nearest-neighbor (J1), next-nearest-neighbor (J2), and third nearest-neighbor (J3) superexchange pathways between six-coordinate cation sites in $La_3Ni_2SbO_9$.

the crystal is Sb-rich, meaning that any Ni^{2+} cations that are present will have relatively few NN Ni^{2+} cations to which they can couple. Consequently their antiferromagnetic interactions with cations on the twelve next-nearest-neighbor sites or the six third NN sites, parametrized by J_2 and J_3 respectively, will not be negligible, and the spin structure based only on NN interactions will not survive into these regions. The *B*-site ordered perovskites Ca_2NiWO_6 and $SrLaNiSbO_6$[14,19,20] provide extreme examples of this situation, with the third and second NN interactions dominating and leading to Néel temperatures of 52.5 and 26 K, respectively. The magnetic moments of the Ni^{2+} cations on these more distant neighboring sites are likely to experience competing interactions and magnetic frustration may then ensue. We propose that the relatively low experimental value of M_{Ni} is attributable to the absence of a spontaneous magnetization in these regions. The presence of antimony-rich regions thus limits the size of the coherent regions of ferrimagnetic order, and causes the formation of domains. If the domains are small the ferrimagnetic order will not be detected in a neutron diffraction experiment, although the atomic moments will all align to give a bulk magnetization in an applied field, as is observed. It is not clear from the available data how large a local fluctuation in composition would be necessary to produce this effect. We note that statistically 8.8% of Ni^{2+} cations will have no Ni^{2+} cations on NN sites, and that only 0.14% have six NN Ni^{2+} cations.

The model described above gives a plausible explanation of the observed properties of $La_3Ni_2SbO_9$. The cation disorder that inevitably results from a 2:1 distribution of cations over two sites that occur in a 1:1 ratio disrupts the magnetic superexchange interactions that would otherwise lead to an ordered spin arrangement throughout each crystallite. Consequently, relatively small magnetic domains form. At low temperatures the bulk magnetic properties of the sample reflect the spontaneous magnetization that is present in each domain, but the magnetic order does not persist over long enough distances to be detected by neutron diffraction. A compound with these properties would usually be classified as a cluster glass, but the origin of the behavior in this case, in a crystalline material with a cation distribution that is ordered in one sense but disordered in another, is so strongly reminiscent of relaxor ferroelectrics that it is justifiable to refer to $La_3Ni_2SbO_9$ as a relaxor ferromagnet. It would be interesting to study the microstructure of the sample to determine the size distribution of the domains; Davies and Akbas[7] have suggested a domain size of ~3−7 nm for analogous relaxor ferroelectrics. Electron microscopy and small-angle neutron scattering are among the techniques that could be used to study this compound further.

It would also be interesting to look for similar behavior in other perovskite materials. Franco et al. have recently studied[21] $La_3Co_2SbO_9$ and observed a different temperature dependence of the magnetization. They also observed a 012 magnetic Bragg reflection in a neutron diffraction pattern collected at 2 K. It is clear that the cobalt and nickel analogues behave differently, suggesting that the physical properties are sensitive to the size or electron configuration of the magnetic cation. Alternatively, the differences might be attributable to different degrees of sample homogeneity, on a microscopic scale, that in turn stem from differences in the synthetic procedures used. In contrast to monoclinic $La_3Co_2SbO_9$ and $La_3Ni_2SbO_9$, $Sr_3Fe_2TeO_9$, containing d^5:Fe^{3+} and d^{10}:Te^{6+}, has tetragonal symmetry at room temperature.[22,23] Interestingly, although the two previous studies of this compound agree on the space group symmetry, they report differing degrees of Fe/Te disorder over the two six-coordinate sites. Again, this might be caused by the use of different synthetic protocols. Ivanov et al.[23] report Fe:Te ratios of 0.72:0.28 and 0.61:0.39 on the two sites for a sample that is said to be ferrimagnetic below 260 K, with a magnetization of 0.03 μ_B per iron atom at 50 K. The function M/H is field dependent at temperatures in excess of 300 K and shows a maximum at a field-dependent temperature between 50 and 100 K. When measured in a field of 100 Oe, the data collected under ZFC and FC conditions differ at temperatures below 260 K; this was the basis for the assignment of the Curie temperature. Ivanov et al. discussed the effect of antisite defects on the magnetic behavior and accounted for the low-temperature maximum in M/H in terms of a re-entrant spin-glass transition. It is perhaps possible that the field dependence above 300 K is caused by the presence of a magnetic impurity and that the hysteresis observed below 260 K is due to the presence of blocked spin clusters in a paramagnet that does indeed behave as a spin glass below the susceptibility maximum; the FC susceptibility shows no sharp rise at 260 K, as might be expected in a ferrimagnet. However, support for the interpretation proposed by Ivanov et al. comes from the fact that they were able to fit their low-temperature diffraction patterns using a magnetic structure in which NN antiferromagnetic superexchange was dominant, albeit with ordered magnetic moments much lower than would be expected for Fe^{3+}. The sample of $Sr_3Fe_2TeO_9$ studied by Augsburger et al. had Fe:Te occupancy ratios of 0.57:0.43 and 0.9:0.1 on the two six-coordinate sites. It showed a well-defined ferrimagnetic transition at 717 K, with a saturation magnetization of 0.8 μ_B per f.u. at 2 K. Neutron diffraction provided convincing evidence for the presence of an ordered magnetic moment on the Fe^{3+} cations, although the magnitude, 0.85 μ_B per Fe atom, was again low. Augsburger et al. referred to the importance of

dx.doi.org/10.1021/ic400675r | Inorg. Chem. 2013, 52, 6648−6653

iron-rich regions for the establishment of long-range magnetic order, as did Ivanov et al. The former attributed the low value of the ordered moment to the competition between Te^{6+} and Fe^{3+} for the electron density on the oxide ions, with the Fe−O−Fe superexchange being weakened as a result. It is not clear why the Curie temperature is as high as 717 K if this explanation is valid. The saturation moments measured by magnetometry for both samples of $Sr_3Fe_2TeO_6$ are lower than would be predicted by the model developed above to account for the behavior of $La_3Ni_2SbO_9$.

Studies of compounds in which the diamagnetic *B*-site cation has the electron configuration d^0, rather than d^{10}, have revealed behavior comparable to that of $La_3Ni_2SbO_9$, but always with some important differences. $Sr_3Fe_2MoO_9$, for example, has been studied in detail by Viola et al.[24] The compound is tetragonal, and the distribution of cations over the six-coordinate sites is the same as in $La_3Ni_2SbO_9$. Magnetic transitions are apparent at 280 and 60 K, and hysteresis is seen at low temperatures, although the magnetization is low (0.15 μ_B per f.u.) and an almost linear function of field at 2 K in fields up to 30 kOe. Neutron diffraction data collected below 250 K could be modeled assuming antiferromagnetic coupling between NN Fe^{3+} cations, the ordered moment at 2 K being ∼1.35 μ_B per Fe^{3+}. This value is low, but higher than those reported for $Sr_3Fe_2TeO_9$. Viola et al. considered the consequences of domain formation in $Sr_3Fe_2MoO_9$ and suggested that magnetic coherence is maintained between some iron-rich regions, thus giving rise to magnetic Bragg peaks but with a reduced mean value for the ordered moment per cation. They argued that the complete absence of this coherence would lead to an absence of a bulk magnetization, whereas a small magnetization was recorded. This argument is valid if the external magnetic field is unable to rotate the net magnetization of the incoherent domains and hence align them. We propose that such a rotation does occur in $La_3Ni_2SbO_9$ and suggest that the domain size is larger in $Sr_3Fe_2MoO_9$ and that the larger domain size hinders the rotation of the magnetization but allows the observation of magnetic Bragg scattering.

It is then possible to develop a model that accounts for $La_3Ni_2SbO_9$, $Sr_3Fe_2TeO_9$, and $Sr_3Fe_2MoO_9$. In each compound atomic disorder on the six-coordinate sites causes the formation of small, magnetically ordered domains. The magnetization of the smallest domains can be rotated by a magnetic field, but the ordering cannot be detected by neutron diffraction. As the domain size grows, the magnetized domains become more difficult to align, but the ordering can be detected by diffraction. We are thus suggesting that the domain size increases in the order $La_3Ni_2SbO_9 < Sr_3Fe_2TeO_9 < Sr_3Fe_2MoO_9$.

CONCLUSION

The apparent inconsistency between the high saturation magnetization of $La_3Ni_2SbO_9$ and the absence of magnetic Bragg scattering in the neutron diffraction pattern has been accounted for in a self-consistent manner by assuming that the cation disorder within the structure results in the formation of small ferrimagnetic domains that are too small to give rise to magnetic Bragg scattering but can be aligned by an applied magnetic field. It is thus reasonable to describe $La_3Ni_2SbO_9$ as a relaxor ferromagnet.

ASSOCIATED CONTENT

Supporting Information

Further details are given in Figures S1−S2. This material is available free of charge via the Internet at http://pubs.acs.org.

AUTHOR INFORMATION

Corresponding Author

*E-mail: peter.battle@chem.ox.ac.uk.

Notes

The authors declare no competing financial interest.

ACKNOWLEDGMENTS

We are grateful to E. Suard for experimental assistance at ILL Grenoble.

REFERENCES

(1) Hill, N. A. *J. Phys. Chem. B* **2000**, *104*, 6694−6709.
(2) Anderson, M. T.; Greenwood, K. B.; Taylor, G. A.; Poeppelmeier, K. R. *Prog. Solid State Chem.* **1993**, *22*, 197−233.
(3) Cox, D. E.; Shirane, G.; Frazer, B. C. *J. Appl. Phys.* **1967**, *38*, 1459−1460.
(4) Todate, Y. *J. Phys. Chem. Solids* **1999**, *60*, 1173−1175.
(5) Battle, P. D.; Gibb, T. C.; Herod, A. J.; Kim, S.-H.; Munns, P. H. *J. Mater. Chem.* **1995**, *5*, 865.
(6) Cussen, E. J.; Vente, J. F.; Battle, P. D.; Gibb, T. *J. Mater. Chem.* **1997**, *7*, 459.
(7) Davies, P. K.; Akbas, M. A. *J. Phys. Chem. Solids* **2000**, *61*, 159−166.
(8) Bokov, A. A.; Ye, Z. G. *J. Mater. Sci.* **2006**, *41*, 31−52.
(9) Cowley, R. A.; Gvasaliya, S. N.; Lushnikov, S. G.; Roessli, B.; Rotaru, G. M. *Adv. Phys.* **2011**, *60*, 229−327.
(10) Kimura, T.; Tomioka, Y.; Kumai, R.; Okimoto, Y.; Tokura, Y. *Phys. Rev. Lett.* **1999**, *83*, 3940−3943.
(11) Alvarez, I.; Veiga, M. L.; Pico, C. *J. Alloys Compd.* **1997**, *255*, 74−78.
(12) Larson, A.C.; R. B. von Dreele *General Structural Analysis System (GSAS)*, Report LAUR 86-748; Los Alamos National Laboratories: Los Alamos, NM, 1990.
(13) Rietveld, H. M. *J. Appl. Crystallogr.* **1969**, *2*, 65−71.
(14) Attfield, M. P.; Battle, P. D.; Bollen, S. K.; Gibb, T. C.; Whitehead, R. J. *J. Solid State Chem.* **1992**, *100*, 37.
(15) Sesaki, S.; Fujino, K.; Takeuchi, Y. *Proc. Jpn. Acad.* **1979**, *55*, 43.
(16) Jansen, M. *Ang. Chem., Int. Ed. Eng.* **1978**, *17*, 137−137.
(17) Martin, R. L.; Nyholm, R. S.; Stephenson, N. C. *Chem. Ind.* **1956**, 83−85.
(18) Scatturin, V.; Corliss, L.; Elliott, N.; Hastings, J. *Acta Crystallogr.* **1961**, *14*, 19−26.
(19) Lopez, C. A.; Curiale, J.; Viola, M.d.C.; Pedregosa, J. C.; Sanchez, R. D. *Phys. B* **2007**, *398*, 256−258.
(20) Martinez-Lope, M. J.; Alonso, J. A.; Casais, M. T.; Fernandez-Diaz, M. T. *Z. Naturforsch.* **2003**, *58b*, 127−132.
(21) Franco, D. G.; Fuertes, V. C.; Blanco, M. C.; Fernandez-Diaz, M. T.; Sanchez, R. D.; Carbonio, R. E. *J. Solid State Chem.* **2012**, *194*, 385−391.
(22) Augsburger, M. S.; Viola, M. C.; Pedregosa, J. C.; Carbonio, R. E.; Alonso, J. A. *J. Mater. Chem.* **2006**, *16*, 4235−4242.
(23) Ivanov, S. A.; Nordblad, P.; Eriksson, S. G.; Tellgren, R.; Rundlof, H. *Mater. Res. Bull.* **2007**, *42*, 776−789.
(24) Viola, M. C.; Alonso, J. A.; Pedregosa, J. C.; Carbonio, R. E. *Eur. J. Inorg. Chem.* **2005**, 1559−1564.